Geophys. J. Int. (2007) **168,** 90–99 doi: 10.1111/j.1365-246X.2006.03197.x

Strong inhomogeneity beneath Quaternary volcanoes revealed from the peak delay analysis of *S*-wave seismograms of microearthquakes in northeastern Japan

Tsutomu Takahashi,[1,*] Haruo Sato,[2] Takeshi Nishimura[2] and Kazushige Obara[3]

[1] *Department of Geophysics, Graduate School of Science, Tohoku University, Aramaki-aza Aoba* 6-3, *Aoba-ku, Sendai* 980-8578, *Japan. E-mail: ttaka@jamstec.go.jp*

[2] *Department of Geophysics, Graduate School of Science, Tohoku University, Aramaki-aza Aoba* 6-3, *Aoba-ku, Sendai* 980-8578, *Japan*

[3] *National Research Institute for Earth Science and Disaster Prevention,* 3-1, *Tennodai, Tsukuba* 305-0006, *Japan*

Accepted 2006 August 21. Received 2006 August 21; in original form 2006 May 30

SUMMARY

High-frequency *S*-wave envelopes of microearthquakes well reflect the medium inhomogeneity of the Earth. Defining the peak delay time as the time lag from the direct *S*-wave onset to the maximum amplitude arrival of its envelope, we use this quantity to evaluate the strength of multiple forward scattering and diffraction due to random inhomogeneities along the seismic ray path. Analysing peak delay times of many microearthquakes occurred along the subducting Pacific Plate for 2–4, 4–8, 8–16 and 16–32 Hz frequency bands, we find a clear path dependence of the peak delay time in relation to the distribution of Quaternary volcanoes in northeastern Japan. Peak delay times of less than 2 s are usually observed at most of the stations in the study area, but large peak delay times of more than 5 s are observed in the backarc side stations for the case that *S* wave propagates beneath Quaternary volcanoes. The large peak delay times are inferred to be generated at a depth of 20–60 km beneath Quaternary volcanoes by considering ray paths under a 1-D velocity structure. These strongly inhomogeneous regions are located at low-velocity and high *Vp*/*Vs* regions revealed from tomography, which suggests the inhomogeneity may be related to dykes and melts of ascending magma.

Key words: Inhomogeneous media, Scattering, Seismic-wave propagation, Subduction zone.

1 INTRODUCTION

In northeastern Japan, the Pacific Plate is descending beneath the Japan arc from east to west. The volcanic front, a sharp boundary in the distribution of Quaternary volcanoes on the island arc, is located above the 112 ± 19 km iso-depth contour of slab-surface in this area (Tatsumi 1986). Since dense seismic networks have been deployed in this area, detailed structures around this subducting plate have been investigated in many previous studies. For example, an inclined low velocity region that is subparallel to the subducting slab in the mantle wedge beneath the backarc side (e.g. Zhao *et al.* 1992; Nakajima *et al.* 2001) reaches to the Moho beneath the volcanic front. Recently, Tamura *et al.* (2002) pointed out that the along arc variation of thickness and strength of velocity anomaly in this inclined low-velocity region are in good correlation with the Quaternary volcano distribution. Spatial correlation among the volcanic front, seismic velocity structure, hypocentres of low-frequency earthquakes and gravity anomaly has been carefully considered in the modelling of magma genesis and dynamics of slab subduction (e.g. Hasegawa & Nakajima 2004, for detailed review). Umino & Hasegawa (1984) and Tsumura *et al.* (2000) revealed the 3-D structure of *S*- and *P*-wave attenuation from the spectral inversion, respectively, where the attenuation means the apparent attenuation including both intrinsic absorption and scattering losses. Their results are also incorporated into the modelling of underground structure (Nakajima *et al.* 2005).

There have been several attempts to characterize structures of scattering loss and intrinsic attenuation by applying stochastic approaches. Scattering of seismic waves is generated by small-scale velocity fluctuations and/or distribution of small cracks including partial melt while intrinsic attenuation is strongly related to rock properties and temperature (e.g. Sato & Fehler 1998, for detailed review). Analyses of seismic envelope (including its amplitude, duration, temporal decay and so on) in high-frequency range (>1 Hz) are applied to separate these quantities. It is known that impulsive seismic waves radiated from a source are collapsed and broadened as travel distance increases. This property of seismic waves is called envelope broadening, which is considered to be a result of multiple forward scattering and diffraction caused by random

*Now at: Institute for Research on Earth Evolution, Japan Agency for Marine-Earth Science and Technology, Showa-machi 3173-25, Kanazawa-ku, Yokohama 236-0001, Japan.

© 2006 The Authors
Journal compilation © 2006 RAS

inhomogeneities. The general feature of envelope broadening is described well by the Markov approximation of a parabolic wave equation (Sato 1989; Sato & Fehler 1998; Saito *et al.* 2002). The peak delay time (hereinafter called t_p), which is defined as the time lag from the direct wave onset to the maximum amplitude arrival, is known to be a good measure of scattering strength (Gusev & Abubakirov 1999a,b). Duration time of direct-wave envelope including later part of peak arrival also reflects the scattering strength even though we need to consider the intrinsic absorption (Sato 1989; Saito *et al.* 2002). Analysing peak delay times and duration times for *S*-wave envelopes of microearthquakes at frequency bands from 1 to 10 Hz, Obara & Sato (1995) found a significant difference of envelope broadening between the forearc and the backarc side of the volcanic front in Kanto-Tokai area, Japan. Duration and peak delay times of *S*-wave envelopes observed in the backarc side are relatively long especially for higher frequencies but are short and frequency independent in the forearc side. These observations indicate that short-wavelength spectral components of random velocity inhomogeneity are significantly rich in the backarc side. Saito *et al.* (2005) further estimated the power spectral density function of velocity fractional fluctuation and intrinsic attenuation in the forearc side, analysing duration times and maximum amplitudes of envelopes of intermediate depth earthquakes in the northern part of Honshu island, Japan. These previous studies on envelope broadening succeeded in evaluating the stochastic properties of random velocity inhomogeneities; however, their methods presume spatially uniform random inhomogeneities in their target regions but are not used for estimating detailed spatial variation of random velocity inhomogeneities.

In this study, we first carefully examine the peak delay times of *S* waves in relation to travel distance, frequency and spatial distribution of ray paths for shallow- and intermediate-depth microearthquakes occurring around the subducting Pacific Plate in northeastern Japan. Subsequently, we evaluate 3-D spatial variations of scattering strength by applying a simple method using the property of envelope broadening. Finally, we discuss the results with seismotectonic conditions in this region such as the distribution of Quaternary volcanoes.

2 DATA

We analyse velocity waveform data recorded at 100 Hz sampling rate by Hi-net (High Sensitivity Seismograph Network Japan) of the National Research Institute for Earth Science and Disaster Prevention (NIED). Three-component seismometers are installed at the bottom of a borehole at each station (Obara *et al.* 2005). We use waveform data of 262 stations from 393 small and moderate sized earthquakes that occurred around the subducting Pacific Plate, and hypocentre locations of the unified result provided by Japan Meteorological Agency (JMA). Magnitude of the earthquake we analysed is ranging from 2.3 to 5.5. Epicentres, seismic stations and ray paths used in this study are shown in Fig. 1 by circles, dots and grey lines, respectively.

We measure the peak delay time t_p as follows. We first deconvolve recording system response for two horizontal components of velocity seismograms, and calculate root mean square (rms) for the sum of two components in four frequency bands 2–4, 4–8, 8–16 and 16–32 Hz. The envelopes are smoothed by applying a moving time window of which the width is twice the centre period of each frequency band. Then, we measure t_p in seconds for the *S* wave in a 30 s time window starting from the *S*-wave onset (see Fig. 2).

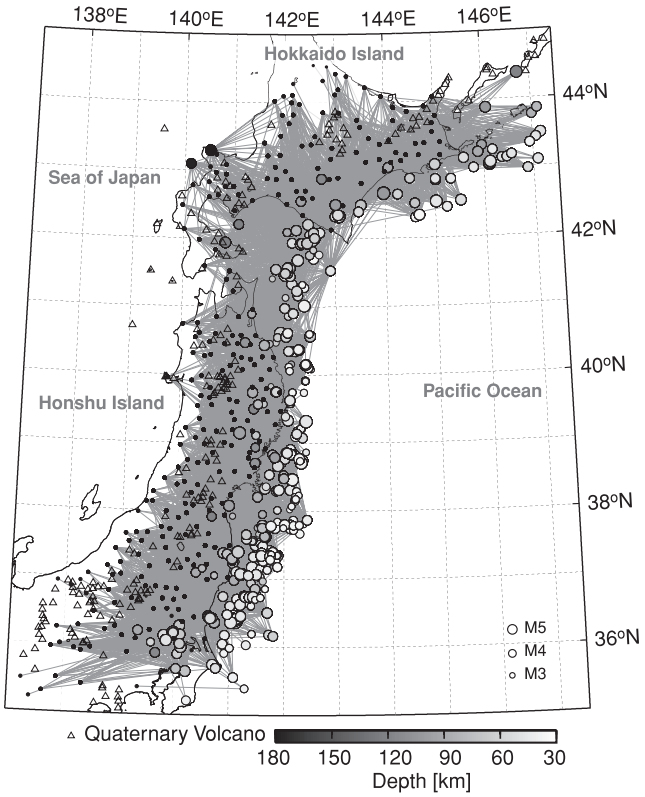


Figure 1. Distribution of seismic stations of Hi-net (dots) and epicentres (circles) used in this study in northeastern Japan arc. The diameter and grey scale of each circle represent the earthquake magnitude and focal depth, respectively. Grey lines are seismic ray paths. Open triangles represent Quaternary volcanoes.

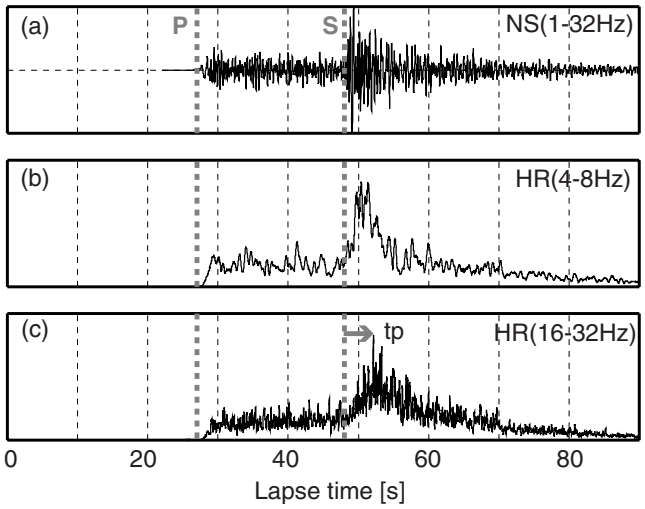


Figure 2. Example of observed seismogram and its envelopes: (a) Velocity seismogram in NS-component in 1–32 Hz band after the deconvolution of recording system response; (b) rms envelope of horizontal components in 4–8 Hz and (c) rms envelope of horizontal components in 16–32 Hz. Vertical grey-dotted lines represent *P*- and *S*-wave onsets and t_p is the peak delay time from the *S*-wave onset.

Some of the waveform data show no clear *S*-wave peaks due to large *P*-coda. We do not use such seismograms in the following analyses. We further restrict the use of data for hypocentral distances from 100 to 250 km because envelope broadening due to scattering does

© 2006 The Authors, *GJI*, **168,** 90–99
Journal compilation © 2006 RAS

not dominate over the source duration time at shorter distances and the travel distance dependence of envelope broadening has different characteristics at longer distances (Sato 1989). As a result, the total number of waveform data we used are 10 738 (2–4 Hz), 11 007 (4–8 Hz), 10 832 (8–16 Hz) and 10 118 (16–32 Hz).

3 TRAVEL DISTANCE DEPENDENCE OF PEAK DELAY TIME

Fig. 3 shows observed peak delay times against hypocentral distances in logarithmic scale for each frequency band. Data for hypocentral distances from 100 to 250 km plotted by black dots clearly show a liner trend. Even though scatter of the data looks large, we find that the peak delay times increase with hypocentral distance increasing. White lines in Fig. 3 represent the linear regression lines of peak delay times against hypocentral distance R in each frequency band. Coefficients of these regression lines show no significant difference among different frequency bands. Here, we define the logarithmic deviation of peak delay time from the regression line (hereinafter $\Delta \log t_p$) as

$$\Delta \log t_p[f] = \log t_p^{\mathrm{obs}}[f] - (A_{\mathrm{dis}}[f] + B_{\mathrm{dis}}[f] \log R), \quad (1)$$

where A_{dis} and B_{dis} are regression coefficients shown in Fig. 3. Fig. 4 shows histogram of logarithmic deviations for each frequency band. The histograms match with a log normal distribution with some skew for each frequency band. The standard deviations are 0.41 for 2–4 Hz, 0.35 for 4–8 Hz, 0.30 for 8–16 Hz and 0.28 for 16–32 Hz, which indicate that the data become less scattered in higher frequency bands.

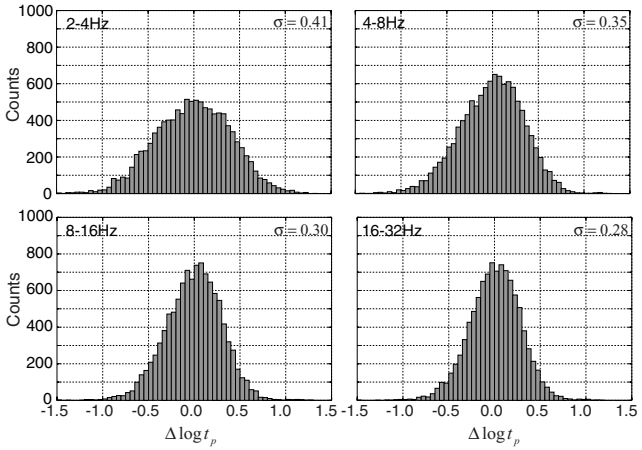


Figure 4. Histogram of logarithmic deviations of *S*-wave peak delay time $\Delta \log t_p$ at each frequency band. Numeral value σ in each bin means the standard deviation.

4 FREQUENCY DEPENDENCE OF PEAK DELAY TIME

The frequency dependence of envelope broadening is one of the most important features to speculate the medium inhomogeneities because of its relation to the power spectral density of velocity fluctuation (Obara & Sato 1995; Saito *et al.* 2002). Following the approach of Obara & Sato (1995), we normalize peak delay times in different frequency bands by the peak delay time in a reference frequency band at each station. Here the 4–8 Hz band is chosen as the

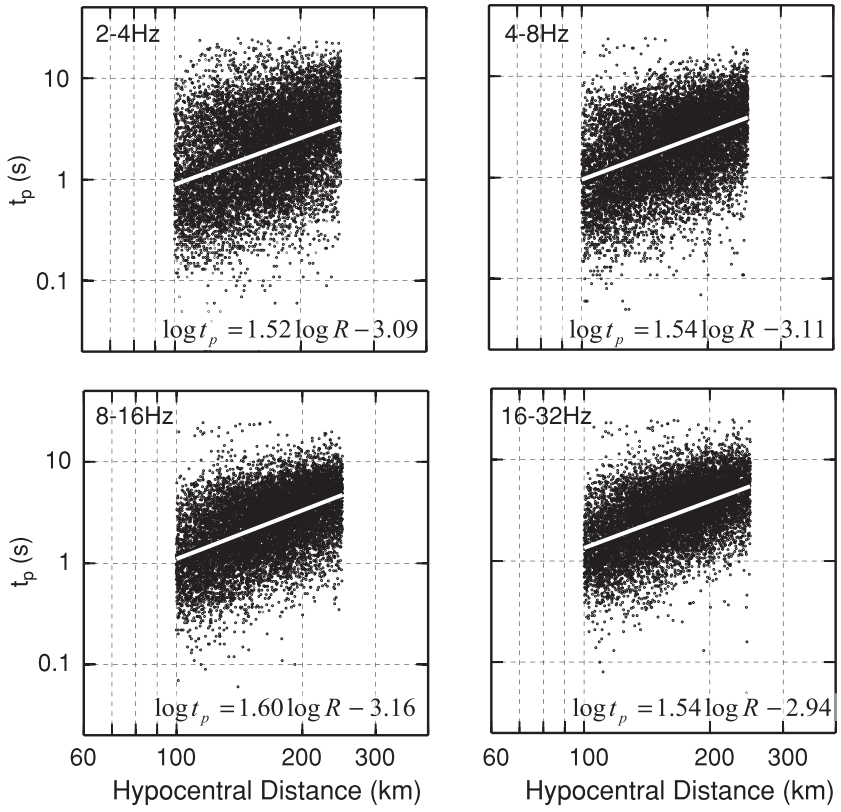


Figure 3. Logarithmic plot of peak delay times against hypocentral distances. Black dots represent the data used in this study. White lines are regression lines.

© 2006 The Authors, *GJI*, **168,** 90–99
Journal compilation © 2006 RAS

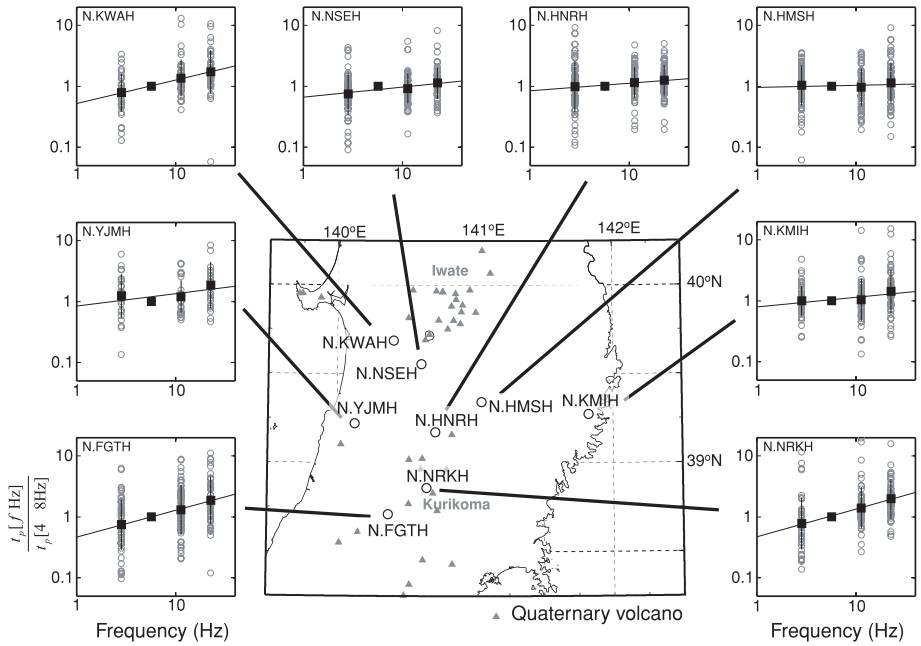


Figure 5. Frequency dependence of peak delay time at stations in central northern Honshu, Japan. Normalized peak delay times are plotted against frequency at each station. Open circles represent observed values and a solid square is the average at each frequency band. Straight line is a regression line at each station.

reference. We evaluate the regression line of the normalized peak delay times against frequency at each station as

$$\log(t_p[f\,\mathrm{Hz}]/t_p[4-8\,\mathrm{Hz}]) = A_{\mathrm{freq}} + B_{\mathrm{freq}} \log f. \qquad (2)$$

The regression coefficient B_{freq} represents the frequency dependence of peak delay times. According to the Markov approximation in random media having von Kármán-type power spectral density function (Saito *et al.* 2002), large B_{freq} corresponds to small power of spectral decay in short wavelength components, in other words, large velocity fluctuation in short wavelengths. As an example, Fig. 5 shows normalized peak delay times $t_p[f\ \mathrm{Hz}]/t_p[4\text{–}8\,\mathrm{Hz}]$ against frequency with a regression line at each station in the central northern Honshu, Japan. Even though the normalized peak delay times are much scattered, there seem to be some spatial variations in the frequency dependence. Two stations in the forearc side (N.KMIH and N.HMSH) have small B_{freq} of about 0.1 while some of the stations in the backarc side (N.FGTH, N.KWAH and N.NRKH) show large values ranging from 0.38 to 0.45 with a clear increase of normalized peak delay time with frequency. However, B_{freq} values at the other stations in the backarc side of non-volcanic area (N.HNRH, N.NSEH and N.YJMH) are as small as those in the forearc side.

We calculate B_{freq} at all of the stations in the study area and then plot them by circles in Fig. 6. In Honshu island arc, stations in the forearc side show small B_{freq} of less than 0.3 and most of those in the backarc side have B_{freq} larger than 0.4. However, stations located on the backarc side between Iwate and Kurikoma volcanoes and between Zao and Bandai volcanoes show small B_{freq} values. The hypocentres are located in the eastern side of seismic stations (see Fig. 1) so that ray paths are dominant in the E–W direction at most of the station in the backarc side. Since the estimated B_{freq} reflects the inhomogeneous structure at the eastern side of each station, we can say that large B_{freq} observed at the stations in the backarc side originate from inhomogeneous structure beneath Quaternary volcanoes. In Hokkaido region, stations only in the backarc sides of Usu and Daisetsu volcanoes show large B_{freq} of more than 0.4 where most of the S waves propagate from south to north. These regional variations of B_{freq} observed in the Honshu and Hokkaido regions imply that the peak delay times for the ray path propagating beneath Quaternary volcanoes tend to show strong frequency dependence.

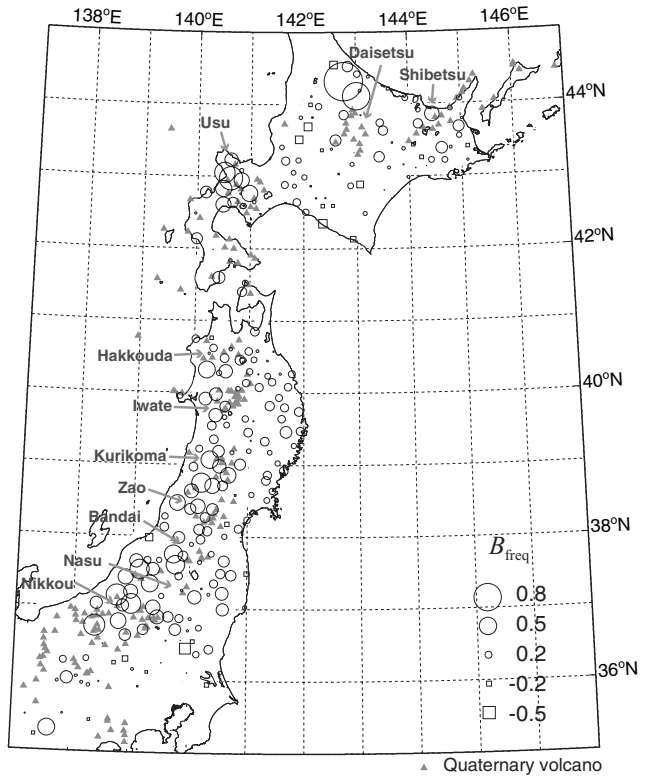


Figure 6. Map view of the frequency dependence of peak delay time in northeastern Japan. The size of circle or square represents the linear regression coefficient B_{freq}. Grey triangles are Quaternary volcanoes.

© 2006 The Authors, *GJI*, **168,** 90–99
Journal compilation © 2006 RAS

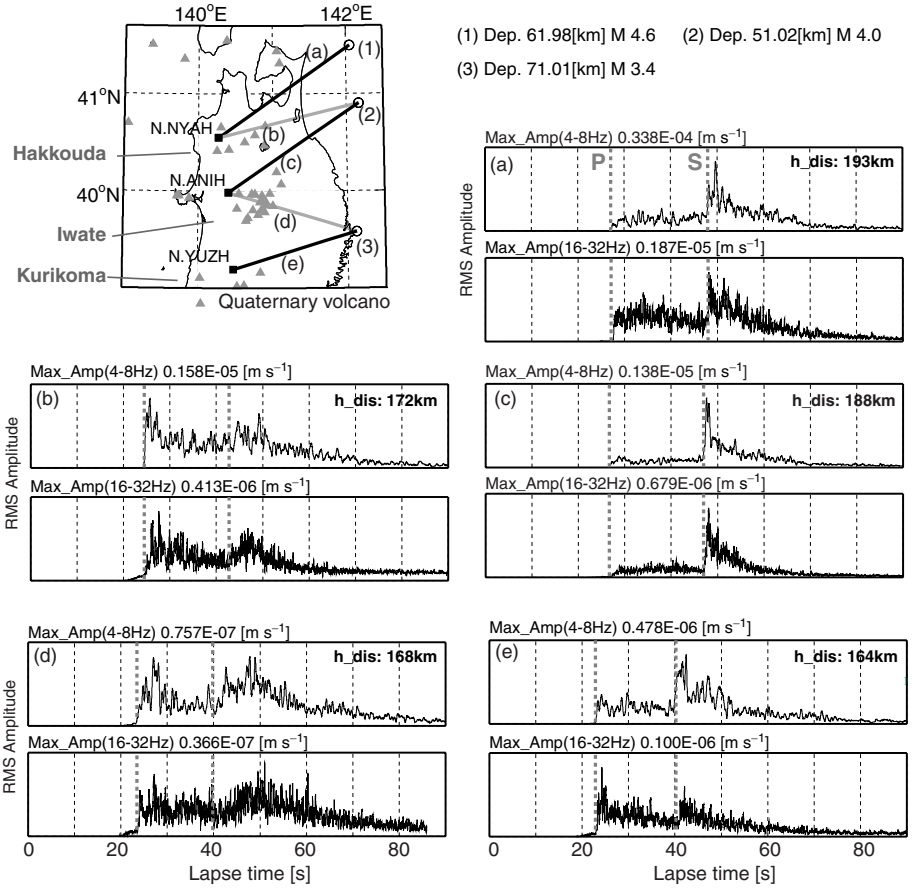


Figure 7. Path dependence of *S*-wave envelopes for three earthquakes (1)-(3) in northern Honshu, Japan. rms envelopes for 4–8 Hz and 16–32 Hz observed on five ray paths are shown. Grey-dotted lines in envelopes are *P*- and *S*-wave onset times. Grey lines in the inserted map represent paths with long peak delay times. Grey triangles are Quaternary volcanoes. Hypocentral distances are shown on the right top of envelopes.

5 PATH DEPENDENCE OF *S*-WAVE ENVELOPES

We have so far discussed characteristics of the observed peak delay times from the averaged values. However, to determine the locations of strong inhomogeneity producing such large peak delay times, it is also necessary to carefully examine the path dependence of peak delay times at each station. Fig. 7 shows some examples of seismic envelopes observed at stations in the backarc side of the volcanic front in northern part of Honshu island for the microearthquakes beneath the Pacific Ocean. The envelopes for the two frequency bands of 4–8 and 16–32 Hz are shown. Although Obara & Sato (1995) reported strongly broadened envelopes in the backarc side of the volcanic front in Kanto-Tokai area, it is clearly recognized that the envelopes on three ray paths numbered (a), (c) and (e) (black lines) show small peak delay times for both 4–8 and 16–32 Hz. This observation strongly suggests an existence of weak inhomogeneities along these ray paths. The envelopes on ray paths numbered (b) and (d) (grey lines) indicate large peak delay times at higher frequency bands. From the visual inspection of *S*-wave envelopes in the study area, the ray paths propagating beneath Quaternary volcanoes tend to show larger peak delay times, and those propagating only through non-volcanic areas show small peak delay times even in high-frequencies. Similar path dependence is observed for most of the study area including Hokkaido island.

In the forearc side of the volcanic front in our study area, most of the *S*-wave envelopes show small peak delay times as reported in Kanto-Tokai area (Obara & Sato 1995). However, we find that *S*-wave envelopes propagating beneath western Hidaka region in the forearc side in Hokkaido tend to show large peak delay times. Fig. 8 shows examples of the envelopes observed in this region. The ray paths shown with grey lines have large peak delay times for both 4–8 and 16–32 Hz bands. From the visual inspection of the other envelopes observed in this region, a grey-coloured region in an inserted map in Fig. 8 is estimated to be the locations of strong scattering. The peak delay times of the envelopes propagating through this region are large for all of the frequencies. This characteristic is obvious from B_{freq} values at stations around western Hidaka area, all tend to have small values (Fig. 6).

6 MINIMUM VALUE DISTRIBUTION OF PEAK DELAY TIME

To quantitatively characterize the observed spatial variation in peak delay times at stations, we present a simple method which focuses on their ray paths. The logarithmic deviation $\Delta \log t_p$ given by eq. (1) represents the relative strength of accumulated scattering contribution along each ray path. We note that, when a peak arrival is once delayed by medium inhomogeneities, the peak delay time cannot be shortened even if random inhomogeneities are significantly weak at the other regions along the ray path. That is, a small $\Delta \log t_p$ implies the absence of strong medium inhomogeneity along the ray path from the hypocentre to the station. On the other hand, if a large

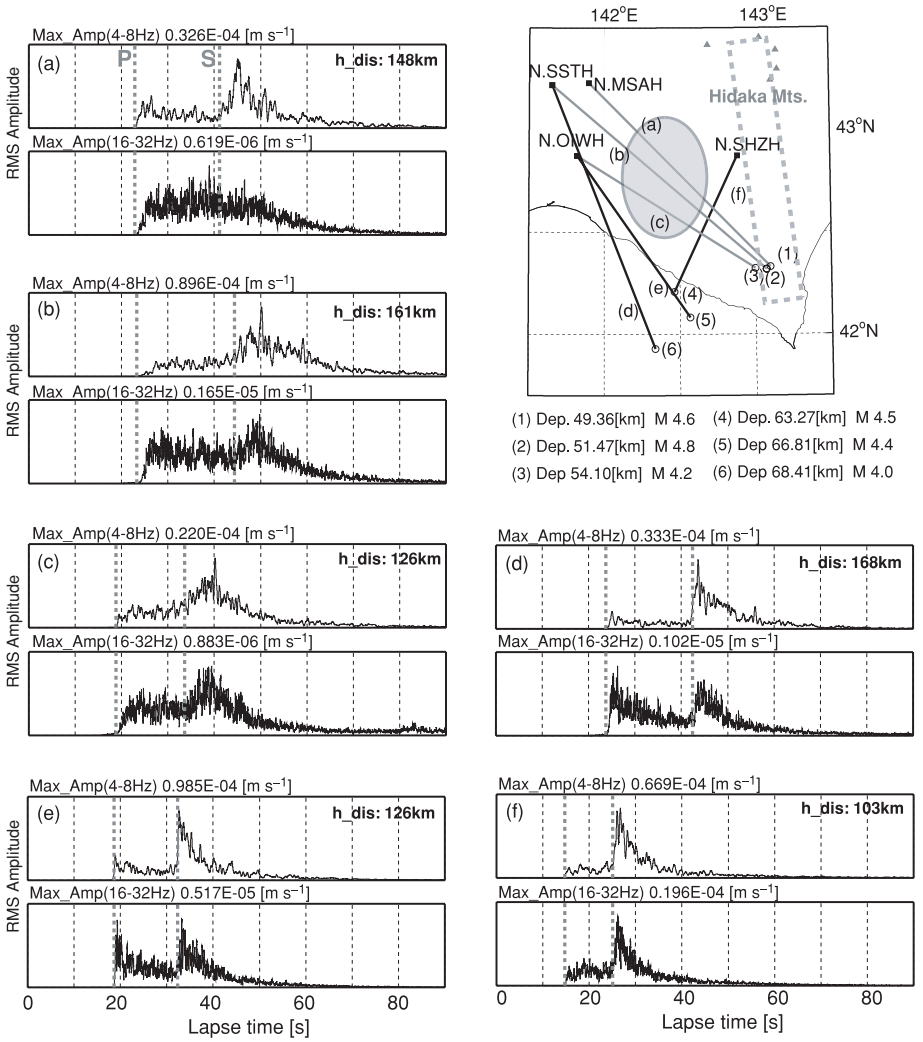


Figure 8. Path dependence of *S*-wave envelopes in the western Hidaka area. rms envelopes for 4–8 and 16–32 Hz observed on six ray paths are shown. Grey-dotted lines in envelopes are *P*- and *S*-wave onset time. Grey lines in the inserted map represent long peak delay times. Grey triangles are Quaternary volcanoes. Hypocentral distances are shown on the right top of envelopes.

$\Delta\log t_p$ is observed, strongly inhomogeneous regions are located somewhere along the ray path.

Let's consider a relation of $\Delta\log t_p$ to the distribution of inhomogeneities in another way by dividing the whole medium into many blocks. Consider one block through which many ray paths propagate and each ray path indicates different values of $\Delta\log t_p$. In this case, the smallest $\Delta\log t_p$ is a representative for characterizing the scattering strength of inhomogeneity of the block, and large $\Delta\log t_p$ should be attributed to the other blocks on its ray path. As a consequence, by allotting the minimum value of $\Delta\log t_p$ to each block, we can speculate about the spatial variation of medium inhomogeneities.

Before showing the result of minimum value distribution of $\Delta\log t_p$, we examine the effect of source mechanism for $\Delta\log t_p$ by using 134 earthquakes of which focal mechanisms are determined by broad-band seismic network (F-net) of NIED (Okada *et al.* 2004). The magnitude and focal depth ranges of these events are 3.5–5.5 and 35–120 km, respectively. Assuming double couple radiation pattern of *S* wave from each source, we compared the radiation pattern coefficient $|R^S_{\theta\phi}|$ and $\Delta\log t_p$ for each frequency bands (Fig. 9). Although the scatter of data is large, by taking the average of $\Delta\log t_p$ in each bin with class interval 0.1 of $|R^S_{\theta\phi}|$, we can confirm that the dependence on radiation pattern is negligibly weak for all frequency bands.

The minimum-value distribution of $\Delta\log t_p$ in northeastern Japan is evaluated as follows. We divide the study region into many small blocks of which the size is $0.10^\circ \times 0.10^\circ$ in horizontal and 20 km in depth. Seismic ray paths are calculated under a 1-D velocity structure of Hasegawa *et al.* (1978). We first measure the minimum value of $\Delta\log t_p$ for each block. And then, we take an average of the minimum values over nearest nine blocks in horizontal direction to smooth the spatial variation of $\Delta\log t_p$. Fig. 10 shows the minimum value distributions of $\Delta\log t_p$ for 2–4, 4–8, 8–16 and 16–32 Hz at depths of 0–60 km. Blocks of small $\Delta\log t_p$ values, which correspond to weak inhomogeneities, are indicated by white or yellow colours while blocks of large $\Delta\log t_p$ values by red or black colours. The blocks crossed by more than or equal to five ray paths are shown in the figure, and other blocks are masked by grey colours. If the number of ray paths having a long-travel distance (>80 km) from source to block is less than 5, we also masked such blocks by grey colour because envelope broadening due to scattering will not be dominant at short-travel distances. The maximum number of

© 2006 The Authors, *GJI*, **168,** 90–99
Journal compilation © 2006 RAS

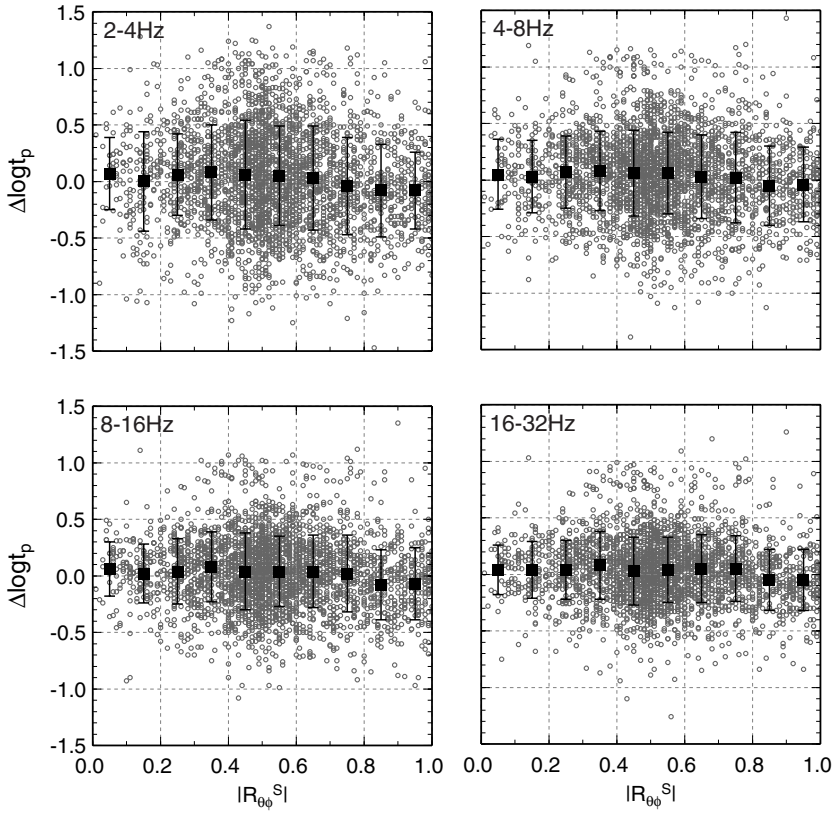


Figure 9. Logarithmic deviation of peak delay time against source radiation pattern coefficient $|R^S_{\theta\phi}|$. Open circles are observed data. Black squares and error bars represent average and the standard deviation of logarithmic deviation of peak delay time in each bin with class interval 0.1 of $|R^S_{\theta\phi}|$.

rays propagating through a block is 508, and 65 per cent blocks in the study area contain more than 20 ray paths.

At the 2–4 Hz band, most of the Honshu and Hokkaido regions show small $\Delta\log t_p$ values of less than -0.5 at 0–60 km in depth except for 20–40 km in depth beneath the western Hidaka and 20–60 km in depth beneath the Daisetsu area (the name of each region is shown in Fig. 5 and 7), and a region around 41°N and 142°E (hereafter, we call this region eastern Aomori) in the forearc side. The results for the 4–8 Hz band show large $\Delta\log t_p$ values at a depth of 40–60 km beneath Iwate volcanic group, even though the other regions show similar features with those for the 2–4 Hz band. At the 8–16 Hz band, some of the regions in the backarc side indicate relatively large values at a depth of 0–20 km. Such strong scatterings in the high frequency range observed at the backarc side are consistent to the results of Obara & Sato (1995). However, closely looking at the spatial changes, we can recognize that small $\Delta\log t_p$ values appear beneath gaps of Quaternary volcanoes at a depth of 20–40 km. The strong inhomogeneities beneath Quaternary volcanoes become more significant at 40–60 km in depth, but still we can find weak inhomogeneities beneath the gaps of Quaternary volcanoes similar to the shallower part. The values of $\Delta\log t_p$ in these non-volcanic areas are almost the same with those in the forearc side. Western Hidaka and eastern Aomori regions show large $\Delta\log t_p$ values similar to those in lower frequencies. At the 16–32 Hz band, distributions of large $\Delta\log t_p$ values well match with the locations of Quaternary volcanoes, and especially at 40–60 km in depth, significantly large $\Delta\log t_p$ values appear just beneath Quaternary volcanoes. Contrary to the results at 8–16 Hz, weak inhomogeneities are unclear between the Quaternary volcanoes at 40–60 km in depth.

7 DISCUSSION

Waves are effectively diffracted by velocity inhomogeneity having a scale larger than the wavelength. For example, the wavelength corresponding to the typical frequency of 20 Hz *S* wave is about 200 m. Strong inhomogeneities with a scale from a few hundreds of metres to a few kilometres beneath the Quaternary volcanoes are new findings to interpret the underground structure. These regions are recognized as high *Vp*/*Vs* and low-*Vs* regions from the velocity tomography analysis (Nakajima *et al.* 2001). This suggests that inhomogeneity may be related with dykes and melts of ascending magma. The western Hidaka region shows large peak delay times for the whole frequency bands. This region is not a volcanic area but shows very high seismicity at a depth of 20–40 km (Katsumata *et al.* 2003). The eastern Aomori region showing large $\Delta\log t_p$ values in all of the frequency bands doesn't indicate any velocity anomalies and high-seismicity. Since the trench axis bends near this region, we suspect this region might be strongly inhomogeneous due to the complex tectonic conditions.

For the quantitative discussion of the medium inhomogeneities, it is necessary to develop some inversion analyses. Assuming Gaussian random media, Gusev & Abubakirov (1999a) proposed an inversion method of peak delay times for the depth variation of scattering strength, but their approach cannot consider the frequency dependence of peak delay time. This disadvantage may be fatal to discuss the difference between volcanic area and western Hidaka area. Introduction of von Kármán type random media make it possible to consider the frequency dependence of peak delay time as was done by Saito *et al.* (2005); however, the studies of the Markov

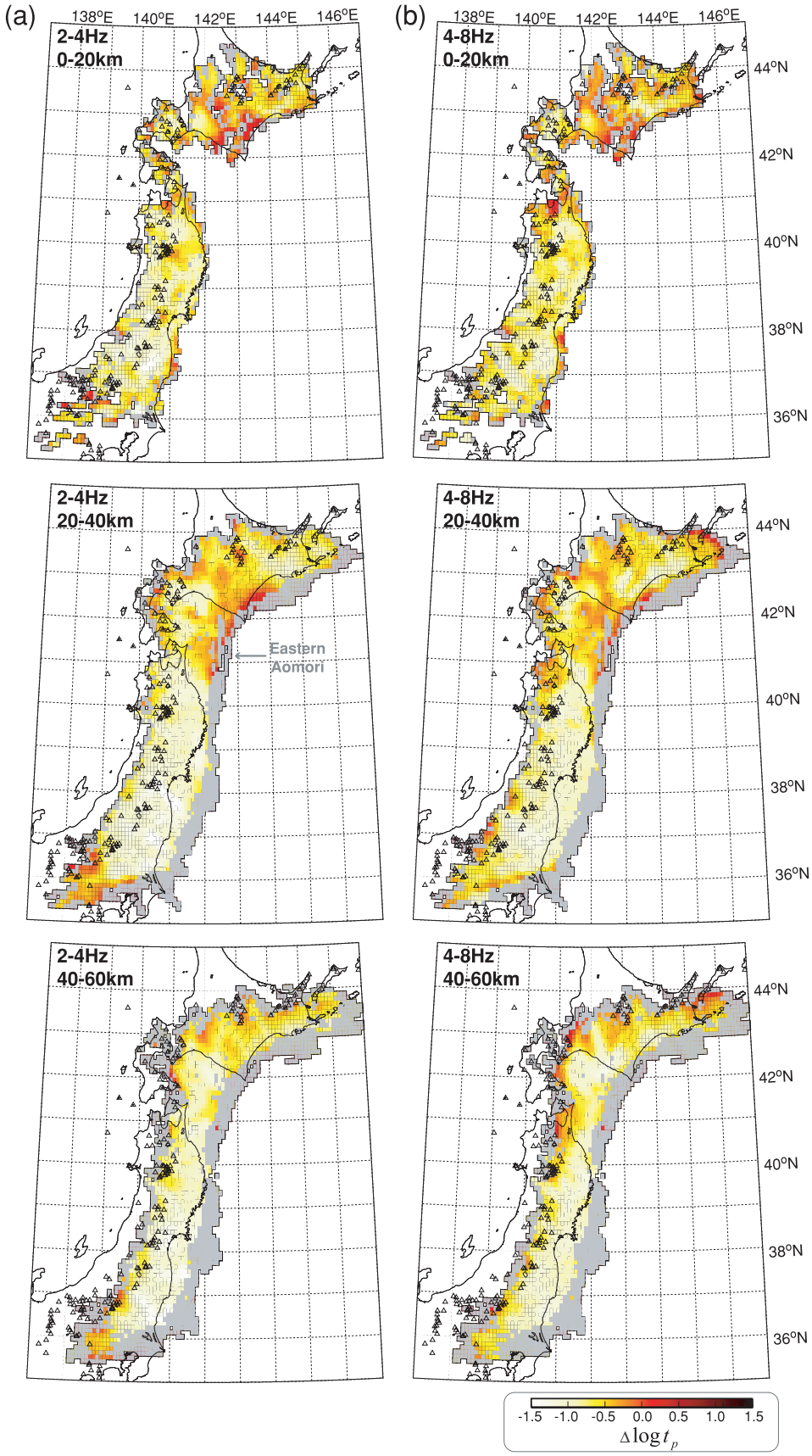


Figure 10. Minimum value distribution of logarithmic deviation of *S*-wave peak delay time $\Delta \log t_p$ in colour scale (a: 2–4 Hz; b: 4–8 Hz; c: 8–16 Hz and d: 16–32 Hz). Grey coloured blocks correspond to those having a few ray paths less than five and those in which the number of ray paths having long-travel distance (≥80 km) from the source to the block is less than five. Open triangles represent Quaternary volcanoes.

© 2006 The Authors, *GJI*, **168,** 90–99
Journal compilation © 2006 RAS

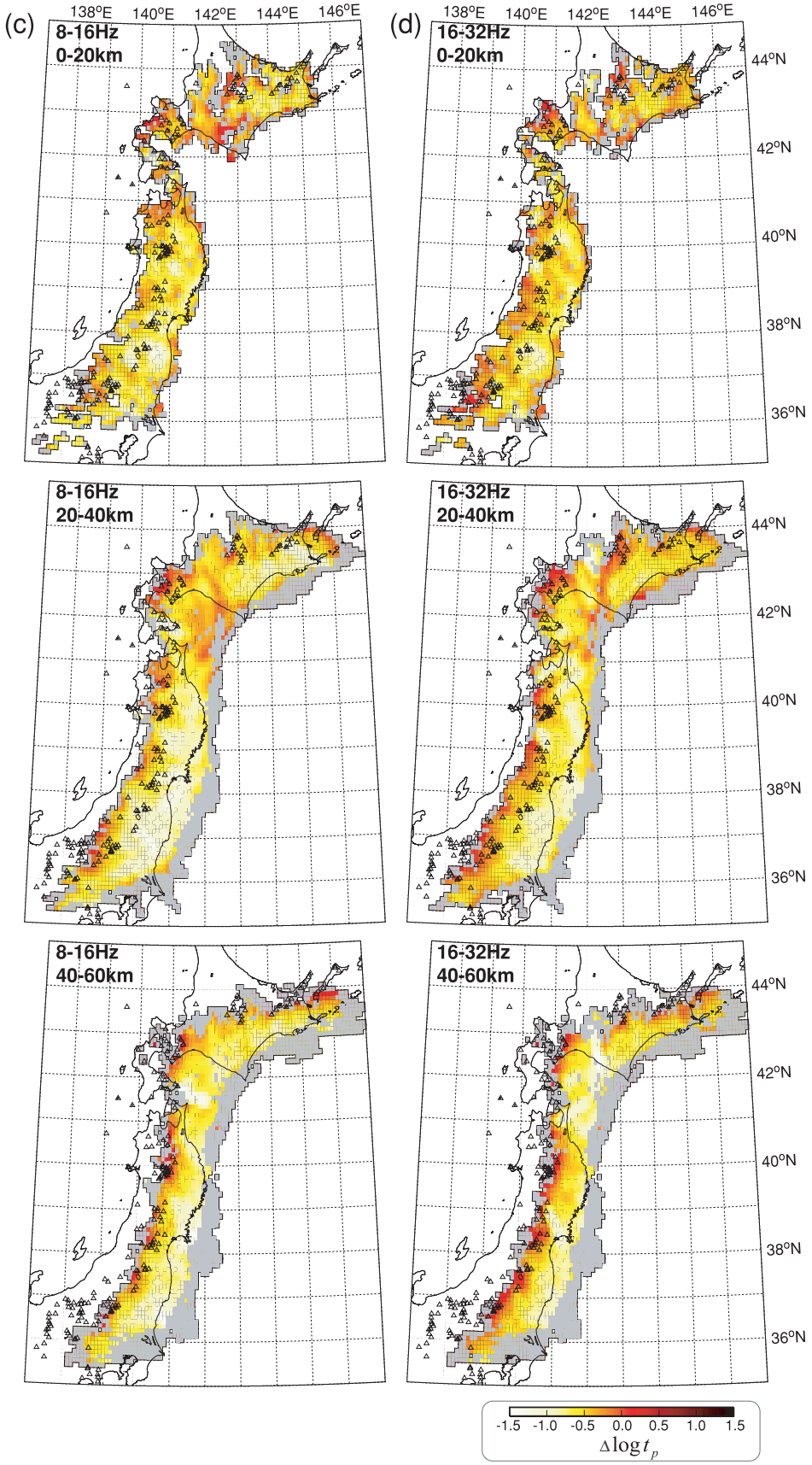


Figure 10. (*Continued*.)

© 2006 The Authors, *GJI*, **168,** 90–99
Journal compilation © 2006 RAS

approximation were established only for spatially uniform random media. An extension of the Markov approximation to the non-uniform case is necessary for this kind of inversion analysis. The peak delay analysis developed here did not pay any attention to absolute amplitudes. It will be necessary to incorporate with the contribution of intrinsic absorption in future.

8 CONCLUSIONS

Examining the path dependence of *S*-wave peak delay times of microearthquakes for frequencies higher than 2 Hz in northeastern Japan, we find that peak delay times observed in the backarc side of the volcanic front show clear path dependence related to the Quaternary volcano distribution. Peak delay times are small at stations in the forearc side of the volcanic front and also in non-volcanic areas in the backarc side; however, large peak delay times are observed only for the ray paths propagating beneath Quaternary volcanoes. Strongly inhomogeneous regions revealed from the peak delay analysis are closely located with the low-velocity and high *Vp*/*Vs* regions, suggesting that the strong inhomogeneities with the scale from a few hundreds metres to a few kilometres tend to concentrate beneath such velocity anomaly regions. Our peak delay analysis gives new information for the quantification of medium inhomogeneity in addition to velocity and attenuation tomography methods.

ACKNOWLEDGMENTS

We thank Stephen R. McNutt of University of Alaska and an anonymous reviewer for their careful reviews and helpful suggestions. We are also grateful to those who made efforts to run the Hi-net and F-net. The hypocentre data of the unified hypocentre catalogue by the Japan Meteorological Agency are used for the analysis. This work is partially supported by the grant in aid for Scientific Research of JSPS #15540399, and the sponsorship of JNES open application project for enhancing the basis of nuclear safety, and the ERI cooperative research programme. This work was conducted as a part of the 21COE programme on Earth Science of Tohoku University. SAC and GMT code are used for data processing and figure plotting.

REFERENCES

Gusev, A. & Abubakirov, I.R., 1999a. Vertical profile of effective turbidity reconstructed from broadening of incoherent body-wave pulses-I. General approach and the inversion procedure, *Geophys. J. Int.,* **136,** 295–308.

Gusev, A. & Abubakirov, I.R., 1999b. Vertical profile of effective turbidity reconstructed from broadening of incoherent body-wave pulses-II. Application to Kamchatka data, *Geophys. J. Int.,* **136,** 309–323.

Hasegawa, A. & Nakajima, J., 2004. Geophysical constraints on slab subduction and arc magmatism, in *The State of the Planet: Frontiers and Challenges in Geophysics,* Vol. 150, pp. 81–94, Geophys. Monogr. Ser., AGU, Washington, DC.

Hasegawa, A., Umino, N. & Takagi, A., 1978. Double-planed structure of the deep seismic zone in northeastern Japan arc, *Tectonophysics,* **47,** 43–58.

Katsumata, K., Wada, N. & Kasahara, M., 2003. Newly imaged shape of the deep seismic zone within the subducting Pacific Plate beneath the Hokkaido corner, Japan-Kurile arc–arc junction, *J. geophys. Res.,* **108,** 2565, doi:10.1029/2002JB002175.

Nakajima, J., Matsuzawa, T. & Hasegawa, A., 2001. Three-dimensional structure of *Vp*, *Vs*, and *Vp*/*Vs* beneath northeastern Japan: implications for arc magmatism and fluids, *J. geophys. Res.,* **106,** 21 843–21 857.

Nakajima, J., Takei, Y. & Hasegawa, A., 2005. Quantitative analysis of the inclined low-velocity zone in the mantle wedge of northeastern Japan: a systematic change of melt-filled pore shapes with depth and its implications for melt migration, *Earth planet. Sci. Lett.,* **234,** 59–70.

Obara, K., Kasahara, K., Hori, S. & Okada, Y., 2005. A densely distributed high-sensitivity seismograph network in Japan: Hi-net by National Research Institute for Earth Science and Disaster Prevention, *Rev. Sci. Instrum.,* **76,** 021 301.

Obara, K. & Sato, H., 1995. Regional differences of random inhomogeneities around the volcanic front in the Kanto-Tokai area, Japan, revealed from the broadening of S wave seismogram envelopes, *J. geophys. Res.,* **100,** 2103–2121.

Okada, Y., Kasahara, K., Hori, S., Obara, K., Sekiguchi, S., Fujiwara, H. & Yamamoto, A., 2004. Recent progress of seismic observation networks in Japan—Hi-net, F-net, K-NET and KiK-net, *Earth Planets Space,* **56,** xv–xxviii.

Saito, T., Sato, H. & Ohtake, M., 2002. Envelope broadening of spherically outgoing waves in three-dimensional random media having power law spectra, *J. geophys. Res.,* **107,** doi:10.1029/2001JB000264.

Saito, T., Sato, H., Ohtake, M. & Obara, K., 2005. Unified explanation of envelope broadening and maximum-amplitude decay of high-frequency seismograms based on the envelope simulation using the Markov approximation: forearc side of the volcanic front in northeastern Honshu, Japan, *J. geophys. Res.,* **110,** B01304 doi:10.1029/2004JB003225.

Sato, H., 1989. Broadening of seismogram envelopes in the randomly inhomogeneous lithosphere based on the parabolic approximation: southeastern Honshu, Japan, *J. geophys. Res.,* **94,** 17 735–17 747.

Sato, H. & Fehler, M., 1998. *Seismic Wave Propagation and Scattering in the Heterogeneous Earth,* Springer Verlag, New York.

Tamura, Y., Tatsumi, Y., Zhao, D., Kido, Y. & Shukuno, H., 2002. Hot fingers in the mantle wedge: new insights into magma genesis in subduction zones, *Earth planet. Sci. Lett.,* **197,** 105–116.

Tatsumi Y., 1986. Formation of volcanic front in subduction zones, *Geophys. Res. Lett.,* **13,** 717–720.

Tsumura, N., Matsumoto, S., Horiuchi, S. & Hasegawa, A., 2000. Three-dimensional attenuation structure beneath the northeastern Japan arc estimated from spectra of small earthquakes, *Tectnophysics,* **319,** 241–260.

Umino, N. & Hasegawa, A., 1984. Three-dimensional Qs structure in the northeastern Japan arc, *J. Seism. Soc. Japan. Ser. 2,* **37,** 217–228 (in Japanese with English abstract).

Zhao, D., Hasegawa, A. & Horiuchi, S., 1992. Tomographic imaging of P and S wave velocity structure beneath northeastern Japan, *J. geophys. Res.,* **97,** 19 909–19 928.